RSC Advances

PAPER

View Article Online
View Journal | View Issue

Cite this: *RSC Adv.*, 2022, **12**, 21056

Rapid photodegradation of methylene blue by laser-induced plasma

Jie Jiang,[a] Na Xie,[b] Yilan Jiang,[b] Jinghua Han, *[a] Guoying Feng,[a] Zhongbing Shi[c] and Changtao He[d]

A new strategy was established for the degradation of wastewater-based organic pollutants. Laser-induced plasma (LIP) was used as an alternative UV light source to realise rapid photodegradation of methylene blue (MB), an organic pollutant. A conventional 1064 nm Nd:YAG laser was used for plasma excitation to degrade MB solutions. The results show that the LIP effectively degraded the organic matter, and the degradation efficiency was related to the UV component with wavelength less than 400 nm. The compositions of the plasma excited by different dielectric substrates are different owing to various mechanisms involving moderate heat dissipation and sonoluminescence. However, metallic substrates, especially Fe, can enhance the proportion of UV light and accelerate the degradation efficiency. In the process of methylene blue degradation, solution parameters, such as initial dye concentration, pH, irradiation time and hydrogen peroxide concentration, will affect the degradation efficiency. The conditions of effective degradation of methylene blue (10 mg L^{-1} MB^{-1} concentration, 50 mL L^{-1} H_2O_2 concentration, pH = 3 and P = 60 mW) were obtained in this study, which can provide reference for practical application.

Received 12th June 2022
Accepted 16th July 2022

DOI: 10.1039/d2ra03633a

rsc.li/rsc-advances

1. Introduction

The issue of water pollution is being exacerbated by rapid industrialisation; in particular, the wastewater generated by the textile printing and dyeing industry contains highly concentrated organic materials and complex components, which cannot be readily degraded.[1] In addition to the problems involving the bright colour of dyes, which can cause unappealing colouration and hinder the penetration of dissolved oxygen into natural water, certain dyes can cause serious medical issues in humans, such as cancer.[2] Therefore, the problem of dye pollution must be urgently addressed. Methylene blue (MB) is a typical organic pollutant found in wastewater discharged by the printing and dyeing factories. Degradation of MB is a key step in the treatment of this particular wastewater.

Traditional methods of organic matter removal from wastewater mostly include physical, chemical, and biological methods, such as adsorption, coagulation, membrane separation, and biological oxidation. Although these traditional methods can effectively degrade organic pollutants, there are usually some problems, such as secondary pollution caused by absorbent recovery, complex coagulation technology, high cost of membrane separation and low efficiency of biological oxidation.[2] Photodegradation has attracted recent attention for the removal of organic pollutants because of its high efficiency and energy-saving potential. Photodegradation technology uses light radiation combined with oxidants, such as hydrogen peroxide and oxygen, to produce hydroxyl radicals that enable the removal of organic matter. This method requires the use of UV light sources.[3] Typically, xenon lamps or mercury vapour high-pressure lamps are used as UV light sources, which emit radiation over a wide range of wavelengths.[4–6] However, the long-term use of UV lamps can cause several problems, including long-term power instability, low photon efficiency, long-term irradiation of pollutants for achieving complete mineralisation, and the presence of harmful mercury.[7,8]

Lasers are in the limelight as alternative light sources that are safe and efficient. However, most studies in this context have been conducted using high-power UV lasers.[9,10] In particular, the photodegradation of dyes by laser-induced plasma (LIP) excited by a 1064 nm laser irradiation medium has not been extensively reported. Owing to its high-temperature-and-pressure characteristics, LIP produces wide-spectrum radiation from UV to infrared (IR), which can be regarded as the conversion of laser energy into wide-spectrum light irradiation. Its UV spectrum can be an appropriate source for decomposition of organic matter. Additionally, LIP is a fully or partially ionised gaseous substance that contains metastable and excited states of atoms, molecules, and particles, which can produce abundant energy.[11] This can considerably improve the efficiency of photodegradation technology.

[a]College of Electronics and Information Engineering, Sichuan University, Chengdu, 610065, China. E-mail: hanjinghua@scu.edu.cn
[b]Laser Fusion Research Center, China Academy of Engineering Physics, Mianyang, 621999, China
[c]Southwestern Institute of Physics, Chengdu, 610041, China
[d]Sichuan Jiuzhou Electric Group Co., Ltd, Mianyang, 621000, China

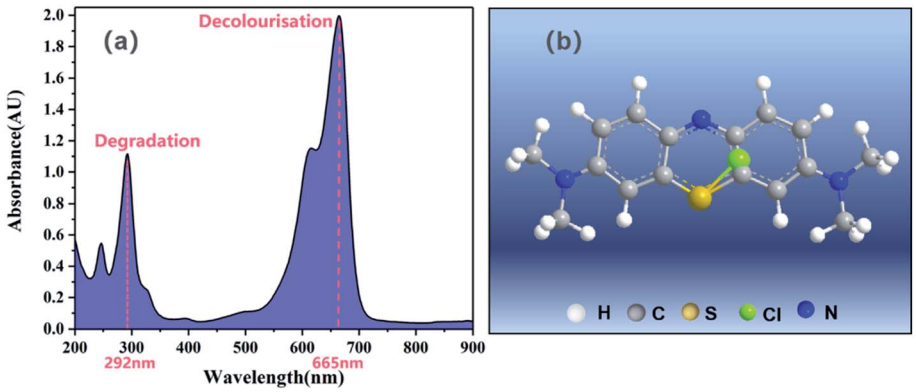

Fig. 1 (a) UV-vis spectra of methylene blue (MB) and (b) its structural formula.[12]

This study was aimed at (1) exploring the possibility of using 1064 nm LIP as a light source for the photodegradation of dyes; (2) establishing the method and principles behind increasing the spectral UV components by comparing the plasma spectral characteristics of the breakdown media; and (3) determining optimal experimental conditions by investigating the influence of environmental factors on degradation efficiency. Therefore, this study can be a reference for LIP-based degradation of hazardous waste.

2. Experimental

2.1. Materials

MB was purchased from Shanghai Aladdin Reagent Research Institute (Shanghai, China). MB is an aromatic compound with the molecular formula of $C_{16}H_{18}ClN_3S$, whose structure is shown in Fig. 1b.[12] MB appears as a solid, tasteless, dark green powder at room temperature, and yields a blue solution when dissolved in water. The UV-vis spectrum of MB in water showed three absorption peaks (Fig. 1a) at 247, 292, and 665 nm. The absorption in the 550–700 nm range can be attributed to a chromophore containing a long conjugated system, whereas the absorption peak at 292 nm can be attributed to aromatic rings.[12] Therefore, the absorbance values at 665 nm and 292 nm were used to evaluate the decolourisation and degradation of MB, respectively. The pH of the solutions was adjusted using 1 mol L^{-1} HCl or NaOH. A UV-vis spectrophotometer (Shimadzu, Kyoto, Japan) was used to determine the dye concentration and the degradation products of MB mixed solution were measured by ICS-90 Ion Chromatograph (Switzerland). Deionised water was used to prepare the experimental solutions.

2.2. Experimental procedure

The experimental setup used in this study (Fig. 2) primarily consists of a 1064 nm neodymium-doped yttrium aluminium garnet (Nd:YAG) laser (Laserver, Wuhan, China), a laser energy meter (Coherent, USA), an optical fibre spectrometer (BIM-6601, Sichuan, China), and a photodegradation reactor. The laser beam was divided into two beams using a beam splitter (Leo-1064-g0032a; Beijing, China), with one being diverted to the

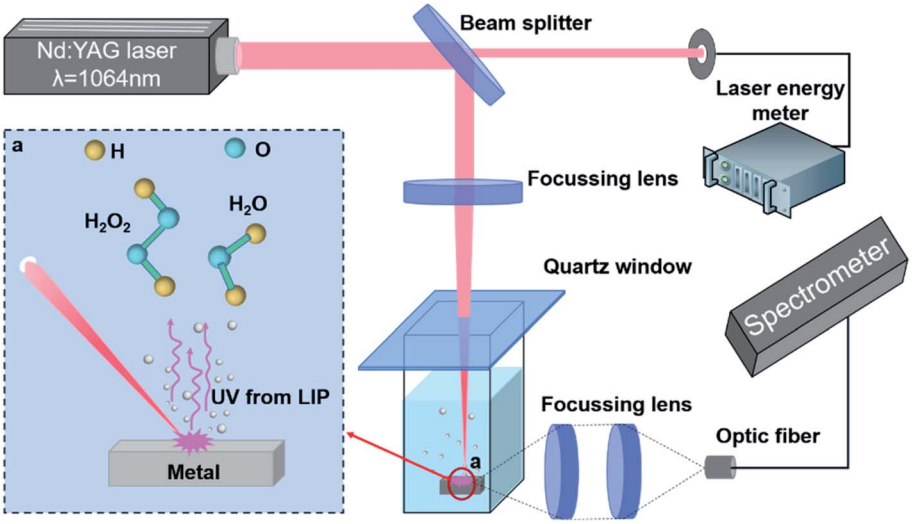

Fig. 2 Schematic diagram of the experimental setup.

laser energy meter for real-time measurement of its intensity, and the other being focussed through a convex lens (GCL-0108, Beijing, China) on a metal plate in a quartz beaker containing the MB solution. In the absence of the metal plate, the beam was focussed onto the centre of the solution. The luminescence signal of the plasma was simultaneously collected by the lateral collection method. When lateral collection was adopted, the collection direction of the plasma radiation was located on the sidewall of the quartz beaker. Two focussing lenses were used to couple the light radiation signal into an optical fibre spectrometer, and the luminous spectrum of the plasma was subsequently obtained using the Brolight software. A 365 nm UV LED lamp (SPN-CLR365, USA) was used as a control to compare the effects of different light sources on the photodegradation of MB.

Prior to the laser irradiation, 50 mL L^{-1} H_2O_2 solution (30%) was mixed with MB at a ratio of 1 : 4 and stirred in the dark for 30 min. The metal sheet was placed in 10 mL of the aqueous MB solution, which was stirred in the dark for 1 min. The concentration of MB in the pristine bulk solution was used as the initial value for the MB degradation measurements. The mixed solution was subsequently irradiated with the laser at a frequency of 20 Hz. The mixed MB solution was separated from the metal plate thereafter and centrifuged at 10 000 rpm for 5 min to eliminate the influence of other impurities. Subsequently, the transparent top portion of the solutions were transferred to quartz cuvettes for measuring their absorption spectra in the wavelength range of 200–900 nm using a UV-2401 spectrophotometer (Shimadzu, Japan). According to the Beer–Lambert law, the concentration of light-absorbing substances linearly varies with the absorbance corresponding to the maximum absorption peak.[13] The concentration of MB (λ_{max} = 292 nm and 665 nm) in the treated solution was determined using a concentration–absorbance calibration curve generated from the absorbance measurements of MB samples at known concentrations. Finally, the degradation products of MB mixed solution were measured by ICS-90 Ion Chromatograph (Switzerland).

2.3. Degradation experiments

In the absence of the hydrogen peroxide oxidizer, the dye was directly irradiated by an unfocussed 1064 nm Nd:YAG laser; plasma excited by a focussed Nd:YAG laser; LIP produced by Al, Cu, and Fe metals; and a UV lamp. MB solutions (20 mg L^{-1}) at identical volumes and temperatures were used in these six groups of control experiments. The time-dependent degradation efficiency of MB was measured using a UV-vis spectrophotometer (Fig. 3).

3. Results and discussion

3.1. Unfocussed Nd:YAG laser for MB degradation

Fig. 3 shows that the removal rate of MB hardly changed with time under these conditions. Degradation and decolourisation rates of only approximately 1% were achieved after illumination for 45 min, and the dye was not removed. The poor degradation and decolourisation were because of the emitted light being in the IR range in the 1064 nm band when the laser was not focussed. Generally, MB undergoes self-degradation in an optical wavelength band of less than 400 nm, because only the UV band induces the formation of hydroxyl radicals in the aqueous MB solutions and enables degradation of organic MB.[14] In conclusion, the dye could not be degraded when the Nd:YAG laser was not focussed.

3.2. Plasma excited by focussed Nd:YAG laser for MB degradation

As shown in Fig. 3, the removal rate of MB increased with time in this scenario. Degradation and decolourisation rates of 29% and 30%, respectively, were achieved after illumination for 45 min. A possible explanation for this behaviour is presented henceforth. The laser irradiation of MB produces LIP (Fig. 4), which has unique physical and chemical properties such as high temperature and high particle kinetic energy. Moreover, the LIP has a conductivity similar to that of metals because it is an aggregate of charged particles. LIP is also prone to chemical reactions owing to its chemical properties, and its

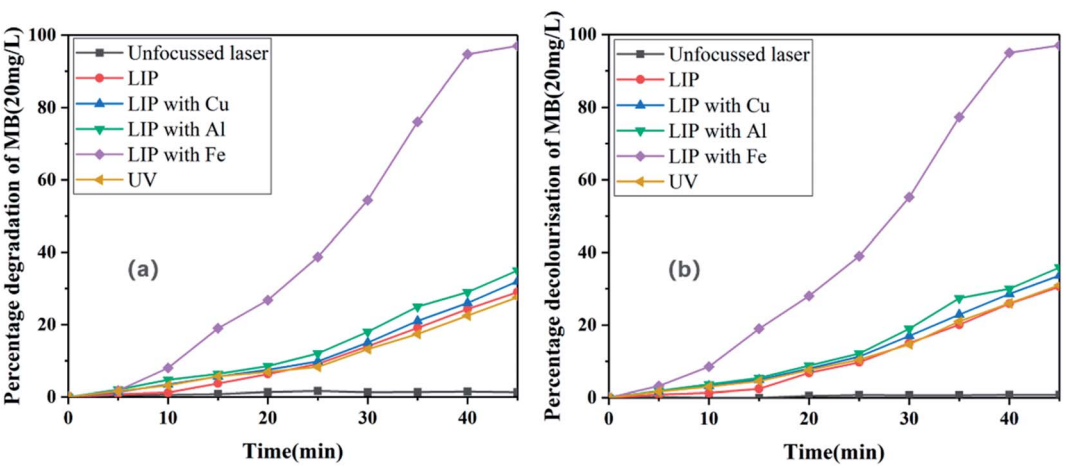

Fig. 3 (a) Degradation and (b) decolourisation of MB dye (20 mg L^{-1}) in the presence of different sources of light irradiation.

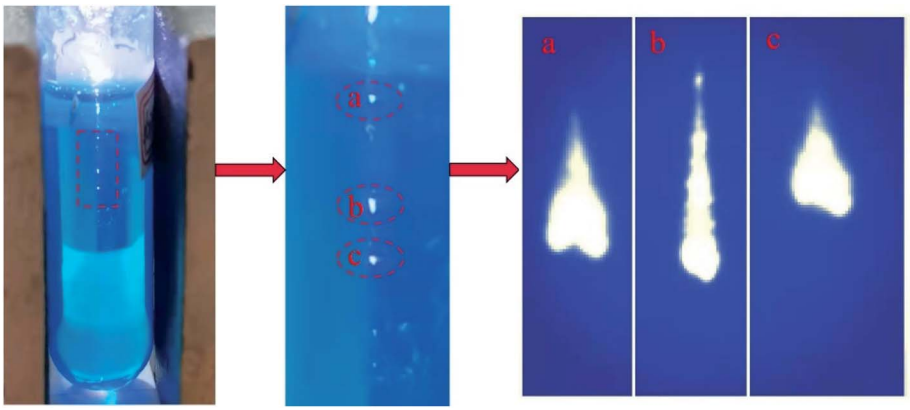

Fig. 4 Plasma in MB excited with laser pulses.

luminescence characteristics can be exploited as a light source.[11,15] Because the spectrum produced by laser plasma is related to the elements and physical properties of the tested sample, the plasma focussed on MB produces less near-UV light than deionized water (Fig. 5a). Therefore, under the action of UV light, the LIP assists the aqueous solution in producing hydroxyl radicals and consequently degrading MB.

3.3. LIP excitation of Cu, Al, and Fe for MB degradation

As shown in Fig. 3, the removal rate of MB increased with time after the addition of the Cu, Al, and Fe metal sheets. Corresponding degradation rates of 32%, 35%, and 97%, respectively, and decolourisation rates of 33%, 36%, and 97%, respectively, were achieved after illumination for 45 min. Higher degradation efficiencies were achieved compared with that of the

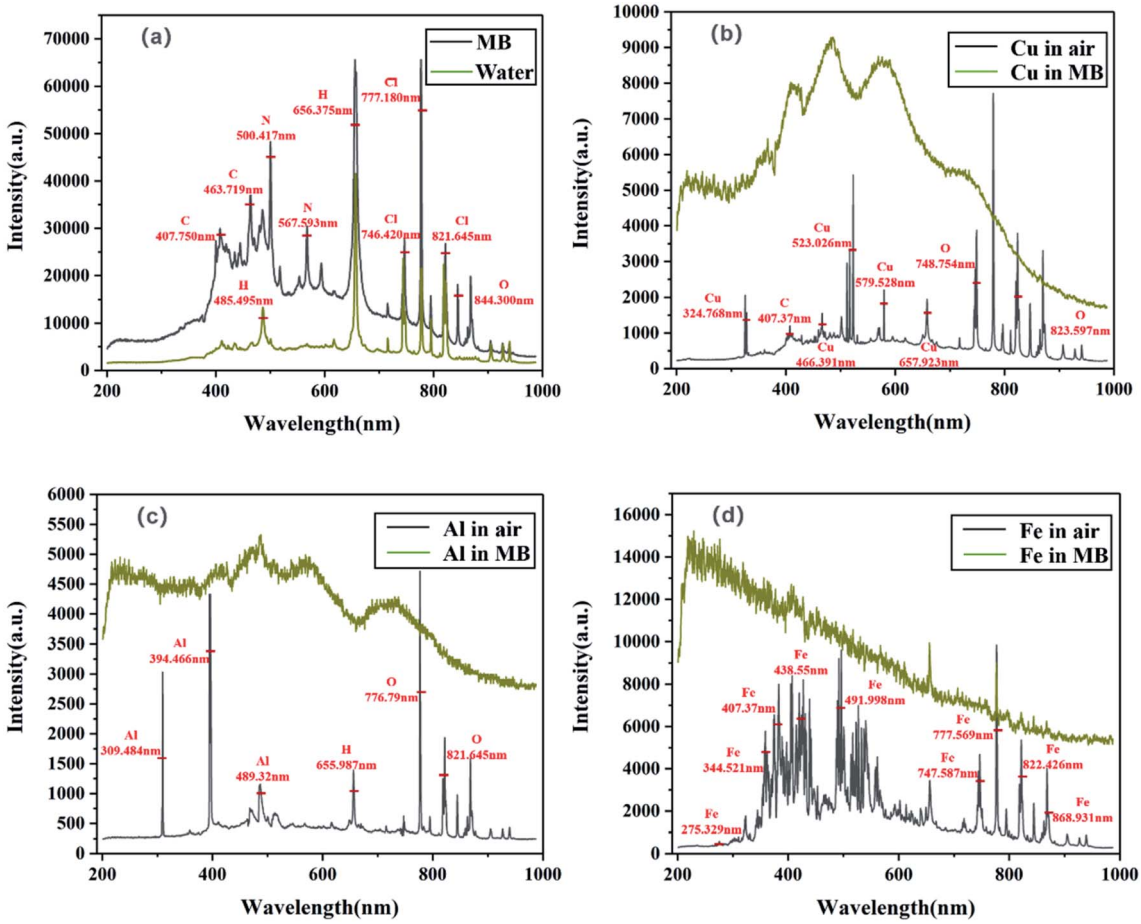

Fig. 5 Luminescence spectrum of (a) MB and water and that of (b) Cu, (c) Al, and (d) Fe in MB and in air.

degradation experiment conducted directly with the LIP, indicating that the addition of a metal plate can promote the degradation of organic compounds. This can be attributed to the more intense UV light generated by the excitation of LIP after the addition of the metal to the dye solution (Fig. 5b–d). Moreover, continuous broadband luminescence spectra were generated by the Cu, Al, and Fe sheets in MB (Fig. 5b–d) presumably because of cavitation produced by the laser pulse in the liquid.[16] Because the bubble generated by a single laser pulse collapses after a period of hundreds of microseconds,[17] semi-adiabatic compression occurs during bubble collapse, resulting in a hot spot with a temperature of the order of 10 000 K. At the end of this period, the bubble can emit a short pulse of light for a picosecond–nanosecond duration, which is known as sonoluminescence.[18,19] This phenomenon typically has broad spectral emission, which can be attributed to ion-electron recombination occurring at the high temperature of the compressed bubbles.[20] Moreover, the reasonably wide wavelength range of the sonoluminescence spectrum in liquids and its high-intensity UV emission are well known.[21] Because water molecules contain hydrogen and have high thermal conductivity, the generated high-temperature and the other ions are easily quenched by water.[22] Therefore, compared with the luminescence spectra of the examined metals in air (Fig. 5b–d), their spectra in water only showed broadband and continuity characteristics, with the atomic and ionic lines being completely quenched at the metal–water interfaces.

In particular, the Fe plate remarkably promoted the degradation of MB compared to that achieved using the Cu and Al plates under identical experimental conditions. Most of the continuous spectral lines generated *via* excitation of Cu in MB were concentrated in the visible region, with only slight fluctuations appearing in the UV region; however, the energy was concentrated in the visible region (Fig. 5b). Although the continuous spectral lines generated by Al excitation in MB considerably fluctuated in the UV region (Fig. 5c), they were also concentrated in the visible region, resulting in dispersion of energy. However, the continuous spectral lines produced by excitation of Fe in MB were concentrated in the UV region, and the highest energy also appeared in the UV region (Fig. 5d). Therefore, compared to Cu and Al, Fe facilitated the production of high-energy UV light in the MB solutions and promoted its degradation. This is possibly because of Fe being a transition metal, the atomic ground state being in the $^5D_4$ orbital, and the outermost electron being a $3d^64s^2$ structure with a partially filled d orbital. Therefore, after the d electrons in the d orbital absorb photons of a certain energy, they transition from a low-energy to high-energy d orbital under the influence of a coordination field and produce an absorption spectrum. This transition is called the d–d electron transition or coordination field transition.[23] Energy-level separation occurs in the coordination field, and both UV and visible light can easily cause electron transitions, resulting in UV and visible spectra. However, Al has a low nuclear charge number and low electron layers, and its coordination energy for accepting lone pair electrons is lower than that of Fe; therefore, Fe exhibits a strong ability for exciting UV light. Although Cu is also a transition metal with coordination field transition, a strong relationship exists between the luminescence spectrum of a metal in solutions and its thermal conductivity.[24] In general, strong continuum emission is a complicated phenomenon that includes Stark and Doppler broadening, bremsstrahlung, compound radiation, and blackbody emission. Therefore, in the case of high-density plasma, blackbody emission is used to explain the observed spectra at the metal–water interface for estimating the surface temperature of the metal in these experiments.[24]

In this study, the heat flux through the metals was dominant because of their high thermal conductivities, and the heat conduction and convection of water were negligible on the nanosecond time scale. Owing to the small heat diffusion length and radiation penetration depth, the heat conduction can be expressed as a one-dimensional equation under the surface-heat-flux boundary condition,[25] as follows:

$$-K\frac{\partial T}{\partial x}|_{x=0} = (1-R_\lambda)I(t) \quad (1)$$

where K is the thermal conductivity, $I(t)$ is the time-dependent incident laser pulse intensity, and $R_\lambda = \frac{(n-1)^2+K^2}{(n+1)^2+K^2}$ is the normal reflectivity of the surface. In this model, local thermal equilibrium was assumed, that is, T(electron) ≅ T(ion) ≅ T(lattice); moreover, melting, vapourisation, and ablation were assumed to occur in the small skin-depth layer (<25 nm) and not significantly affect the heat diffusion process. Based on the aforementioned constant thermal properties, an analytical solution for the transient surface temperature can be obtained using Duhamel's superposition theorem,[25] as follows:

$$T - T_{eq} = \frac{2\sqrt{\alpha}}{K\pi}(1-R_\lambda)\int_0^t \sqrt{t-\tau}\,\frac{\partial I(\tau)}{\partial \tau}\mathrm{d}\tau \quad (2)$$

where T_{eq} is the equilibrium temperature, and α is the thermal diffusivity. The transient temperature, T, was numerically calculated using this model (Fig. 6a). Accordingly, the emission of Fe was found to be more intense than that of Al and Cu owing to its lower thermal conductivity and higher surface temperature. In this experiment, when Fe and H_2O_2 solution were added at the same time, Fe would be oxidized and there was Fenton reaction. However, before and after the experiment, the weight of Fe sheet was compared for many times by electronic balance. It was found that the content of oxidized Fe ion (≅0.0019 mg L^{-1}) in the solution was relatively low compared with the occurrence content of Fenton reaction (≅0.2 mg L^{-1});[26,27] therefore, this experiment only considered the contribution of LIP light of iron metal. In conclusion, compared to Al and Cu, Fe can more effectively enhance the generation of UV light and promote the degradation of MB.

Fig. 6b shows the change of absorption spectra of MB solution with time after LIP irradiation of Fe sheet. The decreases in the values of the two absorbance peaks at 292 nm and 665 nm indicate the degradation of the dye molecule to smaller intermediates such as sulfoxide, sulfone, and sulfonic acid groups.[28] The UV-vis absorption peaks of these compounds are also located in the ranges of 200–300 nm and 500–700 nm, which are similar to those of MB. The detection of these intermediates by

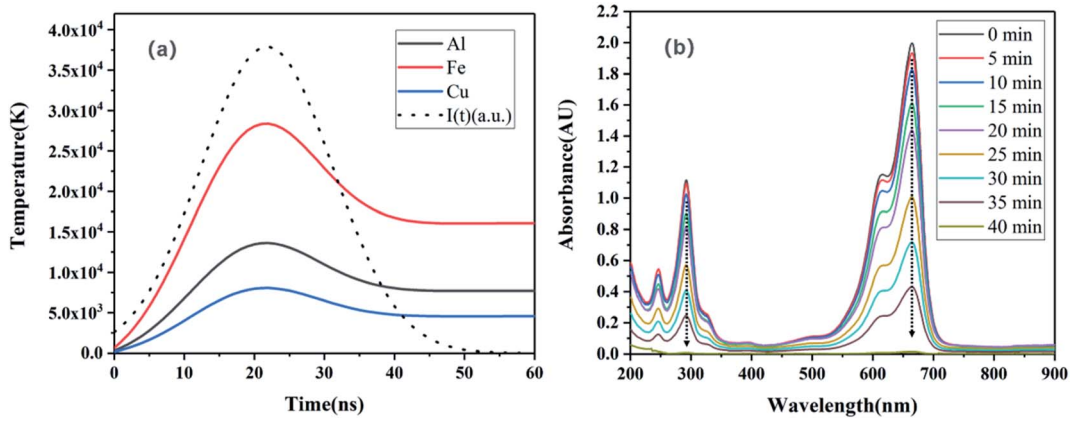

Fig. 6 (a) Transient surface temperature profiles derived using the heat diffusion model. The dashed line indicates the incident intensity $I(t)$ (arbitrary scale). (b) Typical absorbance spectra of MB dye after treatment with Fe under LIP irradiation.

UV-vis spectrophotometry was difficult owing to their low content and the significant overlapping of the absorption spectra. Moreover, no new bands appeared in the UV-vis region during the degradation process, which supports the hypothesis regarding the additional degradation of the intermediate products formed during the dye degradation. Sohrabnezhad *et al.* also reported the phenomenon of a lack of new absorption peaks in the UV-vis region during degradation.[29] Moreover, this phenomenon indicates that MB can be removed under LIP irradiation, and a higher removal rate can be achieved with the assistance of an Fe sheet.

3.4. UV-lamp-assisted degradation of MB

Fig. 3 shows that the removal rate of MB also increased with time in this scenario. Degradation and decolourisation rates of 28% and 31%, respectively, were achieved after illumination for 45 min. The degradation efficiency was lower than that of the experiment in which Fe metal was excited by LIP to produce intense UV light. This is presumably because although the frequency of the LED ultraviolet lamp is high, its photons are emitted without any mode, and the light source is divergent, which results in significant energy loss, and the energy density is 1.0 J cm^{-2}. While the photons of the laser are organised in a coherent manner and emit directionally, a large number of photons are emitted in an extremely small spatial range, resulting in a high energy density of about 1.43 J cm^{-2} and intense LIP-induced UV energy owing to sonoluminescence.[12] Additionally, compared with a UV lamp source, the coherence, monochromatic nature, and high directivity of a laser beam can enable effective absorption of the incident photons and improve the photodegradation rate.

3.5. Photodegradation mechanism

The degradation products of MB measured by ICS-90 Ion Chromatograph are shown in Table 1. Therefore, the major reactions involved in the photodegradation of MB by LIP under laser irradiation are expressed as follows, which are similar to some studies[30–32] and are schematically shown in Fig. 7:

$$H_2O + h\nu \rightarrow H^+ + {}^{\cdot}OH \quad (3)$$

$$H_2O_2 + h\nu \rightarrow 2{}^{\cdot}OH \quad (4)$$

$$R\text{–}S^+ = R' + {}^{\cdot}OH \rightarrow R\text{–}S(=O)\text{–}R' + H^+ \quad (5)$$

$$NH_2\text{–}C_6H_3(R)\text{–}S(=O)\text{–}C_6H_4\text{–}R + {}^{\cdot}OH \rightarrow NH_2\text{–}C_6H_4\text{–}R + SO_2\text{–}C_6H_4\text{–}R \quad (6)$$

$$SO_2 - C_6H_4 - R + {}^{\cdot}OH \rightarrow R - C_6H_4 - SO_3H \quad (7)$$

The production of SO_4^{2-} can be attributed to the continued attack of $^{\cdot}OH$, as follows:

$$R - C_6H_4 - SO_3H + {}^{\cdot}OH \rightarrow R - C_6H_4{}^0 + SO_4^{2-} + 2H^+ \quad (8)$$

The production of NH_4^+ can be attributed to the continued attack of $^{\cdot}OH$, as follows:

$$NH_2\text{–}C_6H_4 - R + {}^{\cdot}OH \rightarrow R - C_6H_4\text{–}OH + NH_2{}^0 \quad (9)$$

$$NH_2{}^0 + {}^{\cdot}OH \rightarrow NH_3 \quad (10)$$

$$NH_3 + H^+ \rightarrow NH_4^+ \quad (11)$$

Other products were gradually degraded and oxidised by the attack of $^{\cdot}OH$ to sequentially produce alcohols, aldehydes, acids

Table 1 Ion chromatography (IC) test data

Ion content (mg L^{-1})					
Experience group	Cl^-	NO_2^-	NO_3^-	SO_4^{2-}	NH_4^+
MB	0.31	—	—	—	—
LIP	2.88	—	0.82	6.12	8.52
UV	3.13	—	2.36	10.80	14.37
LIP-Cu	3.10	—	2.27	11.54	14.05
LIP-Al	3.67	—	3.11	11.72	16.20
LIP-Fe	4.74	—	18.24	12.30	20.71
LIP-Fe/H_2O_2	5.82	—	28.50	13.78	31.64

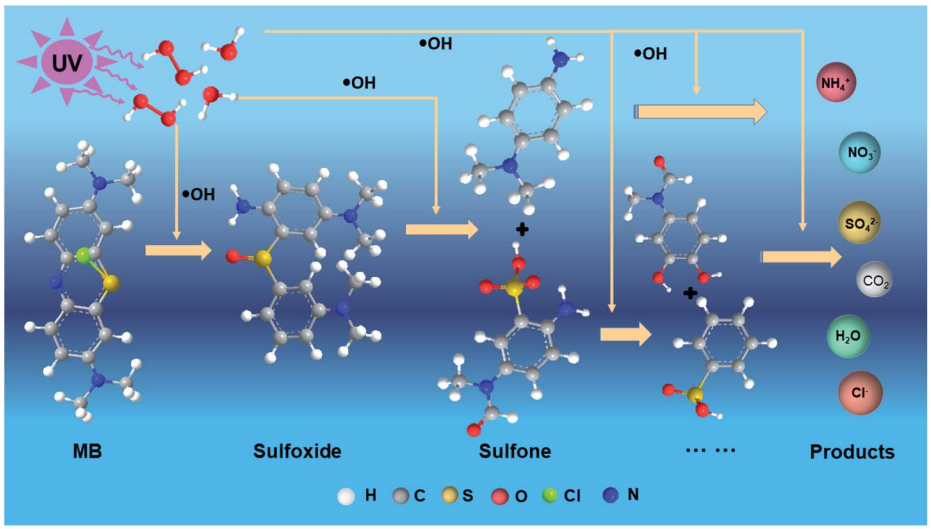

Fig. 7 Schematic diagram of photodegradation of MB.

(*via* spontaneous oxidation), and finally CO_2 (*via* decarboxylation).[30] The general equation for MB degradation can be expressed as follows:

$$C_{16}H_{18}ClN_3S + {}^{\bullet}OH \rightarrow CO_2 + H_2O + NO_3^- + NH_4^+ + SO_4^{2-} + Cl^- \quad (12)$$

The initial step of MB degradation involved the attack of the $^{\bullet}OH$ radical on the C–S^+=C functional group (eqn (5)).[30] Sulfhydryl (–S–) is a chromogenic group of MB, which is electron-absorbing with a relatively high electron cloud density. During UV degradation, it is initially oxidised by the $^{\bullet}OH$ produced by photolysis to generate a sulfonyl group with an absorption wavelength of less than 180 nm (eqn (6)).[33] Therefore, with the progression of the UV degradation reaction, the blue colour of MB gradually fades away to realise its decolourisation and decomposition.

In summary, six different light sources were used to study the degradation of MB. Optimal degradation was achieved when the light generated by the LIP-excited Fe metal was used as the light source. This can be attributed to the sonoluminescence caused by the LIP excitation of Fe, which produced high-density and high-energy UV light, resulting in a faster degradation rate than that in most other experiments.

4. Factors affecting degradation efficiency

4.1. Effects of initial dye concentration

The effects of the initial dye concentration under LIP irradiation were investigated by varying the initial concentration from 10 to 40 mg L^{-1} using an Fe sheet. The time required for complete dye removal increased from 40 to 50 min with increasing initial dye concentration (Fig. 8a and b). These results indicate that the degradation efficiency was inversely related to the initial concentration of the MB dye. Similar results have been reported for the photodegradation of other dyes.[34] A possible explanation for this behaviour is provided henceforth. As the MB concentration increases, the path length of the photons released by the plasma entering the solution decreases, leading to a reduction in the ability of the mixed solution to absorb photons and a decrease in the reaction rate.[14] Hydroxyl radicals are essential oxidants for dye degradation. When the dye concentration increases, more reactants and reaction intermediates react with the hydroxyl radicals, leading to an insufficient number of hydroxyl radicals.[35] Therefore, the degradation rate decreased with increasing dye concentration.

4.2. Effects of initial pH of the dye solution

The solution pH plays an important role in the photodegradation of dyes, because it affects the formation of hydroxyl radicals.[36] The effects of initial pH of the dye solution under LIP excitation of Fe sheet were investigated by varying the pH from 3.0 to 11.0. MB (10 mg L^{-1}) and H_2O_2 (50 mL L^{-1} mixed in a 4 : 1 solution) were used in these experiments. Prior to the irradiation, the initial pH of each experimental solution was adjusted using 1 mol L^{-1} HCl or NaOH and was not controlled during the course of the reaction. Because the aqueous hydrogen peroxide solution exhibits an intense absorption peak between 200 nm and 305 nm,[37] the absorption peak of MB at 292 nm was expected to be affected when the absorbance of the mixed MB-H_2O_2 solution was measured by UV-vis spectrophotometry. Therefore, only the absorption peak at 665 nm was used in this analysis. The experimental results are presented in Fig. 8c. When the pH was increased from 3.00 to 11.00, the degradation of MB was more effective under acidic or alkaline conditions compared to that under neutral conditions. For example, at pH values of 3.0 and 11.0, MB degradation rates of 96% and 66% were achieved within 10 min, respectively; however that at a pH of 7.0 was 32%. This is because under acidic conditions, H_2O_2 is not only derived externally, but can also be generated by

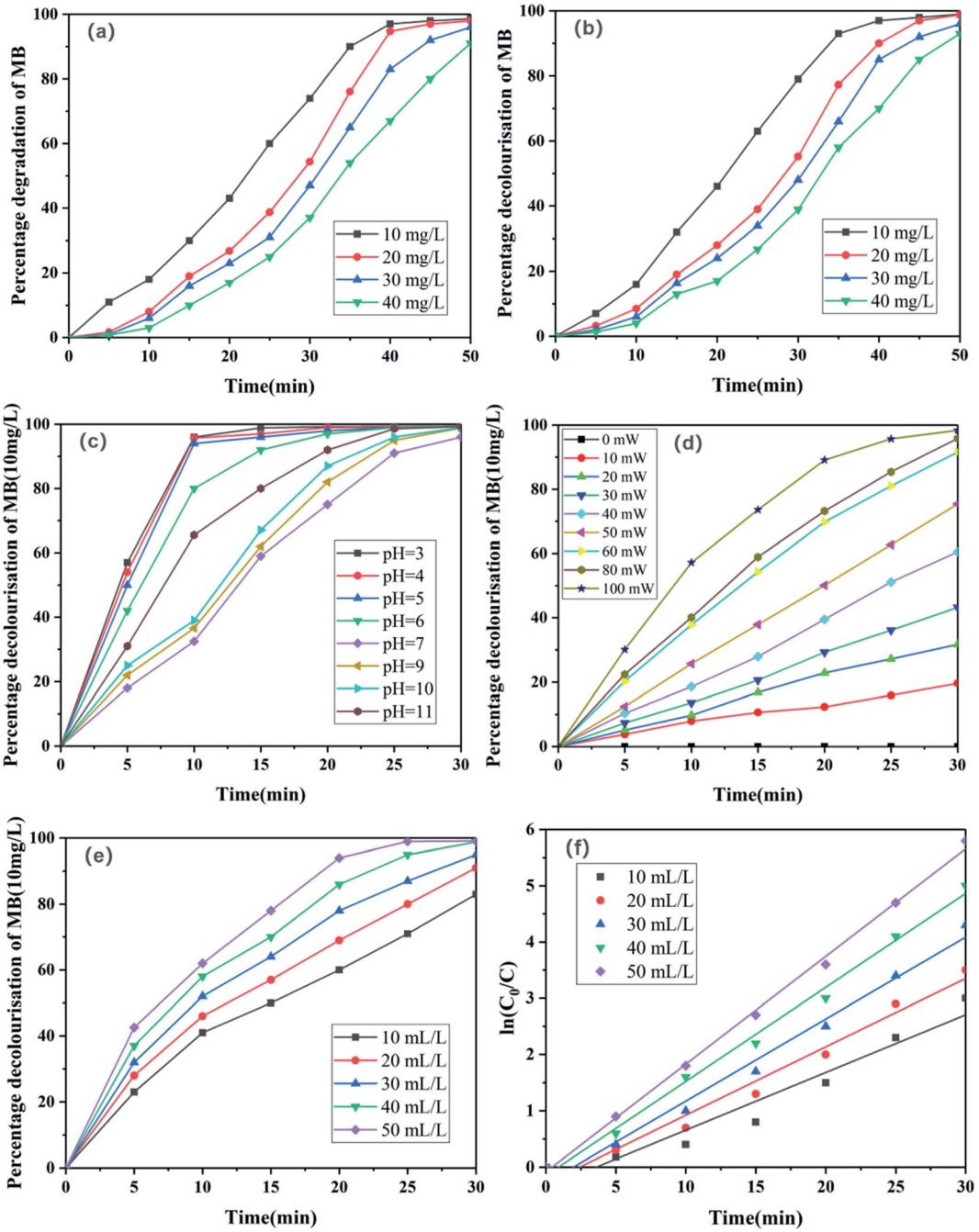

Fig. 8 Effects of MB concentration on its (a) degradation and (b) decolourisation. (c) Effects of pH on decolourisation of MB. (d) Effects of laser energy on decolourisation of MB. (e) Effects of initial H_2O_2 concentration on MB degradation and (f) linear plots of $\ln(C_0/C)$ for the photo-degradation of MB under LIP excitation of Fe sheet.

combining with oxygen because the solution contains abundant H^+ ions, which leads to the generation of more $^{\bullet}OH$ under acidic conditions and superior degradation of MB.[38] However, MB is a cationic dye,[39] and the stability of hydrogen peroxide under alkaline conditions is determined by its pH. The self-decomposition rate of hydrogen peroxide reaches a maximum at a pH of 11–12.[40] Therefore, the removal rates of MB under acidic and alkaline conditions were higher than that under neutral conditions.

4.3. Effects of laser energy

The effects of laser energy on MB degradation are studied by adjusting the output voltage of laser and changing the output power of laser. The results are shown in Fig. 8d. The degradation of MB increased as the laser energy increased. Under the laser energy of 0, 10, 20, 30, 40, 50, 60, 80 and 100 mW, the degradation efficiency at 30 min was 0%, 19.6%, 31.7%, 43.2%, 60.5%, 75.4%, 91.6%, 95.8% and 98.4% respectively. The explanation of this result is that with the increase of laser

Table 2 Degradation rates of MB achieved in various studies

Degradation method	Catalyst	Light source	Power (mW)	Degradation time (min)	Degradation rate (%)	Reference
UV-TiO_2/H_2O_2	1 g L^{-1} TiO_2	Mercury lamp	125 000	10	97	(5)
UV-TiO_2	0.05 g L^{-1} TiO_2	Mercury lamp	125 000	50	100	(14)
Laser-Ag/AgCl	1.2 g L^{-1} Ag/AgCl	Diode laser	1150	10	90	(12)
Visible light-Ag/AgCl	0.6 g L^{-1} Ag/AgCl	Tungsten lamp	100 000	20	98	(29)
Visible light-g-C_3N_4	0.05 g L^{-1} g^{-1}-C_3N_4	Xenon lamp	1000	120	54	(38)
LIP-Fe/H_2O_2	0.02 g L^{-1} Fe	1064 nm Nd : YAG	60	10	99	Present study

energy, the number of photons released increases, and the number of photons absorbed per unit area of MB solution increases, so as to improve the degradation efficiency. However, when the laser energy is too large, the solution will splash, so we control the laser energy of 60 mW in this experiment.

4.4. Effects of initial H_2O_2 concentration

The concentration of H_2O_2 in a photodegradation system can affect photodegradation efficiency.[40] The effects of the initial H_2O_2 concentration (10–50 mL L^{-1}) under LIP excitation of Fe sheet were also investigated. MB (10 mg L^{-1}) was mixed with the different concentrations of H_2O_2 at a ratio of 4 : 1. As mentioned earlier, only the 665 nm absorbance peak of MB was considered because of the presence of hydrogen peroxide in the mixed solution. The results indicate that the degradation of MB was enhanced with a gradual increase in H_2O_2 concentration (Fig. 8e), indicating the importance of H_2O_2 concentration in MB degradation. This is because of the production of hydroxyl radicals by hydrogen peroxide *via* effective oxidation (eqn (4)), and the significant role of $^{\bullet}OH$ in the degradation of MB.[38] A gradual increase in the concentration of H_2O_2 led to an increase in the concentration of $^{\bullet}OH$ *via* decomposition, resulting in an increase in the MB degradation rate with increasing H_2O_2 concentration. Fig. 8f shows linear plots of $\ln(C_0/C)$ corresponding to the photodegradation of MB under LIP excitation of Fe sheet with different concentrations of hydrogen peroxide. C_0 and C are the concentrations of MB initially and at an arbitrary time, respectively. The data suggest that the degradation of MB was consistent with pseudo-first-order kinetics.

In summary, the effects of initial concentration of dye, pH, H_2O_2 concentration and laser energy on photodegradation efficiency were discussed respectively, and the optimal conditions for MB degradation were obtained (10 mg L^{-1} MB^{-1}, 50 mL L^{-1} H_2O_2, pH = 3, P = 60 mW, w = 1.43 J cm^{-2}). A comparison of previously reported research on visible- or UV-light-assisted degradation of nanoparticles (Table 2) indicates that a considerably high degradation efficiency was achieved in this study.

5. Conclusion

UV light generated by LIP was used as a light source to realise the photodegradation of MB as a new strategy for the laser treatment of environmental pollutants. The experimental results show that under optimal conditions, an MB degradation rate of more than 99% was achieved within 10 min of the LIP irradiation. The enhancement of photodegradation efficiency can be attributed to the wide spectrum of light from UV to IR, which accelerates the degradation of organic pollutants owing to the effects of sonoluminescence and high-temperature blackbody radiation. Moreover, the LIP degradation method requires the use of traditional lasers, iron, and a hydrogen peroxide solution, which are incredibly convenient and inexpensive to acquire. In conclusion, the photodegradation conducted using the LIP can be effectively used for environmental applications. Additional research is being conducted on the degradation of MB and other dyes by different metals using lasers with different energies and wavelengths.

Conflicts of interest

The authors declare that they have no known competing financial interests or personal relationships that could have appeared to influence the work reported in this paper.

Acknowledgements

This work was supported by the National Natural Science Foundation of China NSAF(U2030108, U2004162), Sichuan Science and Technology Program (2021YFSY0027) and the Open-Foundation of Key Laboratory of Laser Device Technology, China North Industries Group Corporation Limited(KLLDT202113).

References

1 S. A. Ong, E. Toorisaka, M. Hirata and T. Hano, *J. Hazard. Mater.*, 2005, **124**(1/3), 88–94.
2 N. K. Daud and B. H. Hameed, *J. Hazard. Mater.*, 2010, **176**(1–3), 938–944.
3 J. Liu, N. Ma, W. Wu and Q. He, *Chem. Eng. J.*, 2020, **393**, 124719.
4 B. Yuan, Z. Qian, Q. Yu, R. Hao and Y. Zhao, *Fuel*, 2021, **290**(23), 120026.
5 Q. Zhang, C. Li and T. Li, *Chem. Eng. J.*, 2013, **217**(Complete), 407–413.
6 J. Li, H. Zang, S. Yao, Z. Li and H. Song, *Chin. J. Chem. Eng.*, 2020, **28**(5), 1397–1404.

7 M. Mori, A. Hamamoto, A. Takahashi, M. Nakano and Y. Kinouchi, *Med. Biol. Eng. Comput.*, 2008, **45**(12), 1237–1241.
8 H. Suzuki, S. Araki and H. Yamamoto, *J. Water Proc. Eng.*, 2015, **7**, 54–60.
9 M. Qamar and Z. H. Yamani, *Appl. Catal., A*, 2012, 439–440.
10 M. A. Gondal, M. N. Sayeed, Z. H. Yamani and A. R. Al-Arfaj, *Environ. Lett.*, 2009, **44**(5), 515–521.
11 L. Jin and B. Dai, *Appl. Surf. Sci.*, 2012, **258**(8), 3386–3392.
12 X. Liu, Y. Yang, X. Shi and K. Li, *J. Hazard. Mater.*, 2015, **283**, 267–275.
13 Y. L. Chen, *Opt. Express*, 2013, **21**(6), 7240–7249.
14 E. Bizani, K. Fytianos, I. Poulios and V. Tsiridis, *J. Hazard. Mater.*, 2006, **136**(1), 85–94.
15 L. Jin and B. Dai, *Adv. Mater. Res.*, 2012, **455–456**, 265–270.
16 L. I. Yu-Tong, *Physics*, 2002, DOI: **10.1016/S0731-7085(02)00079-1**.
17 A. Casavola, A. D. Giacomo, M. Dell'Aglio, F. Taccogna and S. Longo, *Spectrochim. Acta, Part B*, 2005, **60**(7), 975–985.
18 Lohse and Detlef, *Nature*, 2002, **418**(6896), 381–383.
19 M. P. Brenner, S. Hilgenfeldt and D. Lohse, *Rev. Mod. Phys.*, 2002, **74**(2), DOI: **10.1103/RevModPhys.74.425**.
20 R. Hiller, S. J. Putterman and B. P. Barber, *Phys. Rev. Lett.*, 1992, **69**(8), 1182–1184.
21 Y. T. Didenko and T. V. Gordeychuk, *Phys. Rev. Lett.*, 2000, **84**(24), 5640.
22 A. D. Giacomo, M. Dell'Aglio and O. D. Pascale, *Appl. Phys. A: Mater. Sci. Process.*, 2004, **79**(4/6), 1035–1038.
23 T. C. Paul, M. H. Babu, J. Podder, B. C. Dev and S. K. Sen, *Phys. B*, 2020, 604.
24 N. Y. S. L. Honoh Suzuki and, *Physchemcomm*, 2002, **5**(13), 88–90.
25 S. Chen and C. P. Grigoropoulos, *Appl. Phys. Lett.*, 1997, **71**(22), 3191–3193.
26 J. C. Chok, Z. B. Hamzah, J. Ma and Y. C. Ho, *IOP Conf. Ser.: Mater. Sci. Eng.*, 2020, **736**, 072013.
27 M. Zheng, C. Xing, W. Zhang, Z. Cheng and S. Zhang, *Inorg. Chem. Commun.*, 2020, **119**(4), 108040.
28 S. Sohrabnezhad, M. A. Zanjanchi and M. Razavi, *Spectrochim. Acta, Part A*, 2014, **130**, 129–135.
29 F. Ronzani, P. Bordat and A. Trivella, *J. Photochem. Photobiol., A*, 2014, **284**, 8–17.
30 A. Ho Ua S, H. Lachheb, M. Ksibi, E. Elaloui, C. Guillard and J. M. Herrmann, *Appl. Catal., B*, 2001, **31**(2), 145–157.
31 H. Shemer and K. G. Linden, *J. Photochem. Photobiol., A*, 2007, **187**(2–3), 186–195.
32 Y. Fang, C. Hu, X. Hu, J. Qu and M. Yang, *Water Res.*, 2009, **43**(6), 1766–1774.
33 K. Hayat, M. A. Gondal, M. M. Khaled, Z. H. Yamani and S. Ahmed, *J. Hazard. Mater.*, 2011, **186**(2–3), 1226–1233.
34 K. Hayat, M. A. Gondal, M. M. Khaled, S. Ahmed and A. M. Shemsi, *Appl. Catal., A*, 2011, **393**(1–2), 122–129.
35 Y. Zhang, J. Liu, D. Chen, Q. Qin, Y. Wu and F. Huang, *Materials*, 2019, **12**(3), DOI: **10.3390/ma12030338**.
36 J. Odo, K. Matsumoto, E. Shinmoto, Y. Hatae and A. Shiozaki, *Anal. Sci.*, 2004, **20**(4), 707.
37 X. Zhao, Z. Ma, F. Qi, Y. Wang and Y. Wang, *Sci. Sin.: Chim.*, 2017, **47**(3), 376–382.
38 Z. F. Liu, Z. J. Liu, L. M. Qie and Z. Y. Yao, *Water Conservation Science and Engineering*, 2020, **6**(3), 1–11.
39 Z. Qiang, J. H. Chang and C. P. Huang, *Water Res.*, 2002, **36**(1), 85–94.
40 H. Shaker, B. Benstaali and N. Al-Bastaki, *Chem. Eng. J.*, 2011, **168**(1), 134–139.